ANNALS OF GEOPHYSICS, 59, FAST TRACK 5, 2016; DOI: 10.4401/ag-7257

PSHA after a strong earthquake: hints for the recovery

L. PERUZZA[1], R. GEE[1,2], B. PACE[3], G. ROBERTS[4], O. SCOTTI[5], F. VISINI[6], L. BENEDETTI[7], M. PAGANI[1]

(1) Istituto Nazionale di Oceanografia e di Geofisica Sperimentale - OGS, Trieste, Italy

(2) Hazard Team, GEM Foundation, Pavia, Italy

(3) DiSPUTer, Università "G. d'Annunzio" Chieti- Pescara, Chieti Scalo, Italy

(4) Department of Earth and Planetary Sciences, Birkbeck, University of London, UK

(5) Institut de Radioprotection et de Surete Nucleaire IRSN, Fontenay-aux-Roses, France

(6) Istituto Nazionale di Geofisica e Vulcanologia, Sezione di Pisa, Italy

(7) Aix-Marseille Université, CEREGE CNRS-IRD UMR 34, Aix en Provence, France

lperuzza@inogs.it

Abstract

We perform aftershock probabilistic seismic hazard analysis (APSHA) of the ongoing aftershock sequence following the Amatrice August 24th, 2016 Central Italy earthquake. APSHA is a time-dependent PSHA calculation where earthquake occurrence rates decrease after the occurrence of a mainshock following an Omori-type decay. In this paper we propose a fault source model based on preliminary evidence of the complex fault geometry associated with the mainshock. We then explore the possibility that the aftershock seismicity is distributed either uniformly or non-uniformly across the fault source. The hazard results are then computed for short-intermediate exposure periods (1-3 months, 1 year). They are compared to the background hazard and intended to be useful for post-earthquake safety evaluation.

I. INTRODUCTION

The event of August 24th, 2016 in Central Italy caused devastating damage and 298 deaths, in spite of the well-known high seismic hazard of the region. The earthquake provoked not only a prompt mobilization of rescue teams but also an unprecedented mobilization of national and international scientific teams. Preliminary scientific data have been progressively provided, complemented and updated [e.g. Gruppo di Lavoro INGV, 2016a, b; Marinkovic and Larsen, 2016; ReLUIS-INGV Workgroup, 2016; GL IREA-CNR and INGV, 2016;ran.protezionecivile.it/IT/dettaglio_evid.php?evid=340867;www.gsi.go.jp/cais/topic160826-index-e.html; www.eqclearinghouse.org/2016-08-24-italy/].

Since August 30th, some participants of the informal *Fault2SHA* working group* opened a forum [http://earthquake2016.prophpbb.com] to circulate ideas, publish material, draft papers and news within the scientific community. This attempt to debate scientific issues in real-time helped to focus investigations in the field, and motivated and boosted this work.

* The WG has been formally approved during the XXXV ESC General Assembly: to join the WG fill the form at https://sites.google.com/site/linkingfaultpsha/fault2sha-esc-wg

Figure 1: *faults and earthquakes overlain on the E-W component of INSAR data [Marinkovic and Larsen, 2016], blue means eastwards; white pins for M>4 before Sep, 28th, 2016 (cnt.rm.ingv.it), dotted for M>5; A=Mt. Vettore Fault, B=Laga Fault, C=Sibillini Thrust.*

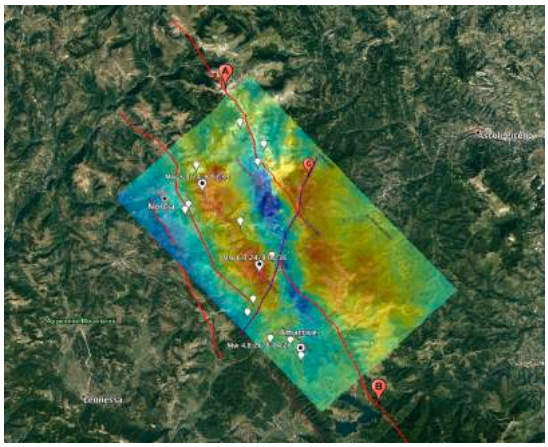

In this paper we gathered pieces of information for a first formulation of aftershock probabilistic seismic hazard assessment (APSHA, as defined by Yeo and Cornell [2009]) in the damaged area. The topography of the area, 3D geometry of the faults and time-dependent estimates of seismicity rates enter in our computations. The results should supersede the standard PSHA practice for the intermediate-term (months to year). Thus, these estimates may be suitable for the impending activities of microzonation, retrofitting and rebuilding. We hope this work will form a basis for gathering more detailed information and to support activities aimed at post-earthquake recovery.

II. Methods

Active normal faulting in the Central Apennines has been recognized for many decades; several authors [e.g. Barchi et al., 1999; Galadini and Galli, 2003; Boncio et al., 2004a, b; Roberts and Michetti, 2004; Benedetti et al., 2013] have described potential seismic sources in the region, which has been recently and historically hit by deadly earthquake sequences. Although fault segmentation, expected magnitude, recurrence time and associated historical earthquakes differ somewhat among authors, there is a clear agreement concerning the lack of surface faulting between the southern termination of Mt. Vettore fault and the northernmost limit of Mt. Gorzano fault (hereinafter Laga fault) where the main shock of the 2016 Amatrice earthquake is located and most of the INSAR deformation is concentrated (Fig. 1).

Figure 2: *surface effects after the 24 Aug earthquake: a) location map of ruptures by EMERGEO WG [2016], Piccardi et al. [2016], Pace et al. [2016]; b) rupture detail at Mt. Vettore.*

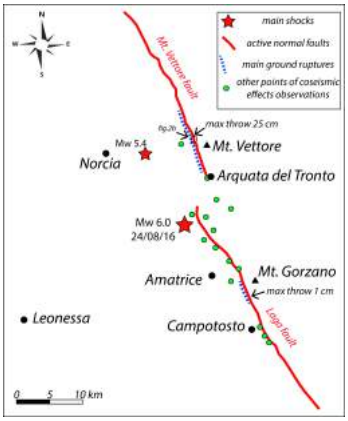

a)

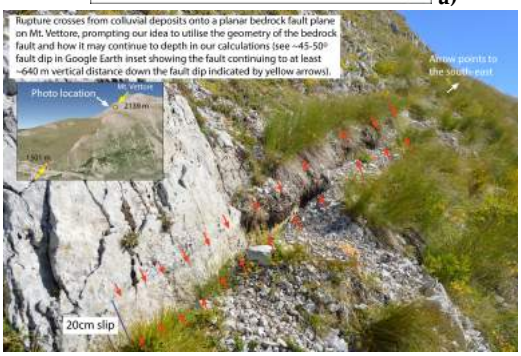

b)

After August 24th, researchers that went into the field documented coseismic ground ruptures with maximum throw up to 25 cm, detectable along segments 3-9 km long (Fig. 2). Most of these surface deformations can be ascribed to coseismic exhumation (rejuvenation)

of existing SW dipping normal faults outcropping along the western flank of Mt. Vettore; minor features were reported also along the Laga fault. The expected magnitude predicted by these displacements and surface rupture length, using existing empirical magnitude vs size relations, is compatible with that of the mainshock, but quite different values (Mw 6.0-6.2, downdip length 4-8 km or more) can be expected due to the uncertainty in the scaling relationship and field measurements. Within the *Fault2SHA* scientific forum, we faced the parameterization of the causative seismogenic source, based on very preliminary and uncertain data, with the aim to discern between the activation of one or more seismogenic sources. As the aftershock sequence evolved, the potential link at depth of Mt. Vettore and Laga faults became more evident: this interpretation is actually the most widely accepted one after the quake (see e.g. Lavecchia et al. [2016]).

Figure 3: *geometry of the fault source proposed for the 2016 earthquake sequence: a) 3D model implemented in OQ; b) surface projection of point sources (black dots) on earthquake locations, fault traces and rupture model; c) fault surface projection on the topography.*

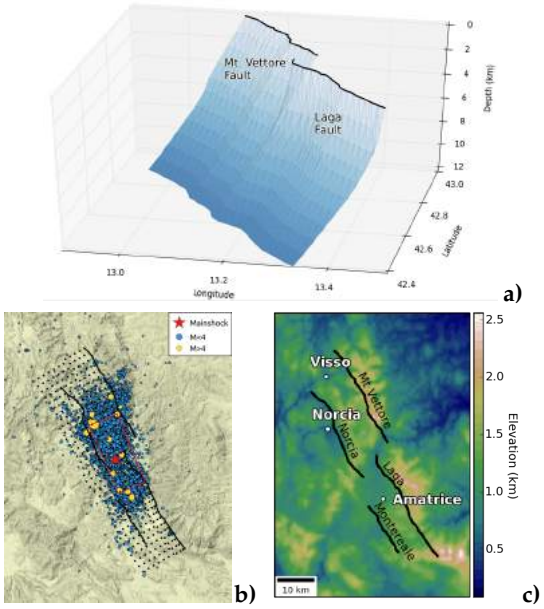

Adopting surface traces based on our mapping activities that acknowledge earlier work on existing published maps, focal mechanisms released from various seismological agencies, and the hypothesis of one unique source, we modeled a SW dipping plane representing a single fault at depth that splits into separate branches towards the surface as the Mt. Vettore and Laga Faults: it represents the preliminary fault geometry for the purpose of our calculations.

This complex fault geometry is one way to explain the two distinct patches of slip distribution obtained by INSAR data inversion located on 50 degree dipping planes [GL IREA-CNR and INGV, 2016]. It is coherent with outcropping observations of two steeper dipping planes (60-70 degrees) separated by about 5 km, in the area between the localities of Arquata del Tronto and Accumuli, where negligible surface expressions have been observed in the field.

The hypothesized fault geometry is compatible with the preliminary aftershock locations, but we do expect refinement and a better resolution when high-quality hypocentral locations will be released. Conversely, this geometry does not account for the alternate stripes of east-westwards movement detected by INSAR (see Fig. 1) for which two distinct conjugate faults may be needed. As these patterns suggesting east-dipping planes are controversial, we decided not to model such a plane in this study. Figure 3a is the 3D sketch of the fault source, created as input for the OpenQuake-engine software [Pagani et al., 2014; OQ, www.globalquakemodel.org/openquake/].

Due to its complex geometry, the surface is represented by a set of point sources (Fig. 3b) on which the global seismicity rate of the fault system is partitioned. The red rectangle roughly corresponds to the rupture area as modeled by GdL INGV [2016a]. Considering the preliminary hypocentral distribution of aftershocks, we limit the fault source to a depth of 12 km,

although the surface itself may extend down to depths of 18 km [e.g. Boncio et al., 2004b].

The basic principle for an APSHA is to treat the earthquake sequence with time-dependent seismicity rates and superimpose it on the traditional Poisson estimate. The traditional PSHA we use as reference is the one stated by law [http://zonesismiche.mi.ingv.it/] since 2004, namely MPS04. For the earthquake sequence, we assume an Omori-Utsu decay of earthquakes with time after the main event. This simple model can be assumed as a realistic one provided that:

- the seismicity belongs to a unique source, with no triggering of nearby cascade events;
- the coefficients are properly calibrated.

We therefore downloaded the INGV bulletin [http://cnt.rm.ingv.it/, data accessed on Sep 17, 2016], for deriving the coefficients of the theoretical model that forecasts the number of events (n) versus time (t) as:

$$n(t) = k/(c+t)^p \qquad (1)$$

where k, c, and p are empirical constants related to a particular aftershock sequence. The fitting was performed by ZMAP code, at www.seismo.ethz.ch/prod/software/zmap/.

A preliminary Gutenberg-Richter (G-R) analysis of this dataset suggests that *b-value* is close to 1, with completeness magnitude at about M2. We fit different sub-samples, by varying the minimum magnitude threshold and learning period: the best candidate by checking the total number events within the longest period available at the time of the analysis, is obtained with $Mmin \geq 1.8$ and 20 days of learning period, represented in Fig. 4a. We are conscious that during the first hours or days small events have probably gone undetected, merged in the coda of bigger events; similarly the completeness and location quality has increased with the deployment of temporary stations. Nonetheless, the coefficients representing Model 1 in Fig. 4a, are suitable to represent the global seismic activity detected during the first weeks, as shown in Fig. 4b, whilst a too rapid decay (black line) is predicted by 10-day learning period only. Finally, we integrate *eq.(1)* to derive the cumulative number of events predicted by the theoretical curve in 30 days, 3 months, and 1 year, starting on October 1st. In Table 1, the number of events and corresponding *a-values* of a G-R distribution are given, assuming $b=1$.

Figure 4: *Omori-Utsu decay for the 2016 sequence: a) fit on the first 20 days of INGV bulletin data with M ≥ 1.8; b) observed versus predicted n(t) from Aug 23 until Sep 16 (24th day), Model 1 of Fig. 4a by light green curve.*

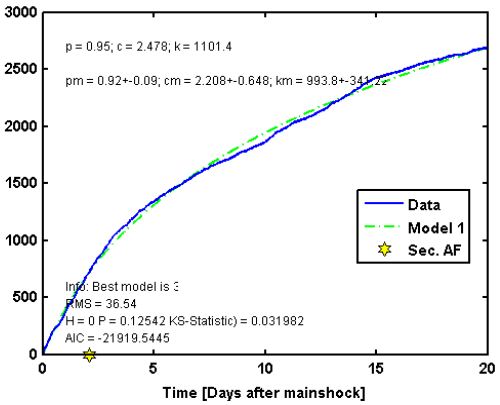

a)

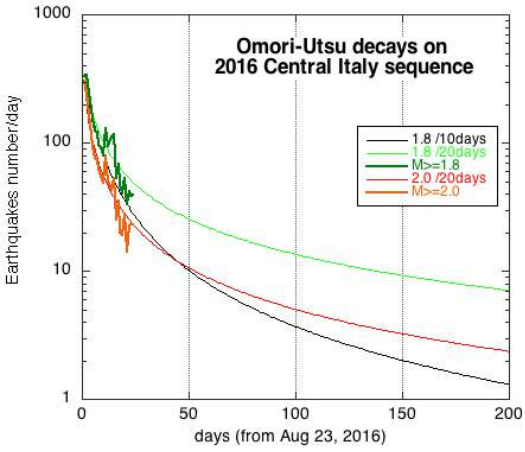

b)

Note that despite the *a-value* increases with time, the seismicity decay is preserved if the prediction time in PSHA is set equal to the observation time of the Omori-Utsu modelling.

With this fundamental limitation (i.e. no extrapolation to other observation times), there is no need to generalize the seismicity rates into non-poissonian earthquake probabilities. Thus in OQ, G-R distributions truncated at *Mmin=3.5* and *Mmax=5.5* (based on magnitude of the largest aftershock) and *a-values* given in Tab. 1 are partitioned on the point sources representing the fault plane.

Table 1: *APSHA, maximum PGA/SA at 10% probability of exceedance in different observation times since Oct, 1st, 2016; values obtained with uniform and non-uniform partitioning of aftershock seismicity rates on the fault.*

Fault Model			PGA /SA(0.3s) (g)	
Time Oct, 1	Num M≥1.8	*a-value (a-year)*	uniform	non-uniform
30 days	745	4.672 (5.751)	0.13/0.22	0.13/0.23
90 days	1597	5.003 (5.605)	0.18/0.34	0.19/0.50
1 year	3236	5.310 (5.310)	0.24/0.47	0.25/0.50

Similarly to Yeo and Cornell [2009], we set uniform and non-uniform partitioning of the seismicity rates: in the second case the *a-value* decreases as a function of distance away from the patches with highest coseismic slip, as it has been observed that aftershocks are often clustered at the ends of faults [e.g. Das and Henry, 2003]. These hypotheses are speculative and uncertainties can be handled as branches of a logic tree. Finally, by applying the new OQ features specifically developed for volcanic areas [Gee et al., 2016], we introduce topography in the computation by defining sites in terms of their 3D location, via a DEM (1km horizontal resolution, Fig. 3c) that results in some minor changes in rupture-to-site distances (*Rrup*). The ground motion prediction equation (GMPE) of Chiou and Youngs [2014] (CY14) is used, because it is defined in terms of *Rrup*; it has been derived using earthquakes from active shallow crustal regions, and is applicable down to *Mw* 3.5. Some examples showing the impact of different ingredients in the APSHA (fault geometry, distance metric, topography, seismicity rate distribution on-fault) are given as Electronic Supplement.

III. Results

We briefly describe here the results in terms of Peak Ground Acceleration (PGA is defined as Spectral Acceleration SA at 0s) and SA(0.3s) for rock sites (Vs30= 800m/s) obtained with the fault aftershock models only (Fig. 5), thus comparing the proxy hazard curve for the 3 observation times with the ones given by MPS04 (Fig. 6).

Figure 5: *APSHA maps showing: a) PGA for rock sites (CY14) at 10% in 1 year from October 1, 2016, using uniform and non-uniform rates with topography; b) the same but SA (0.3s) in the next 3 months.*

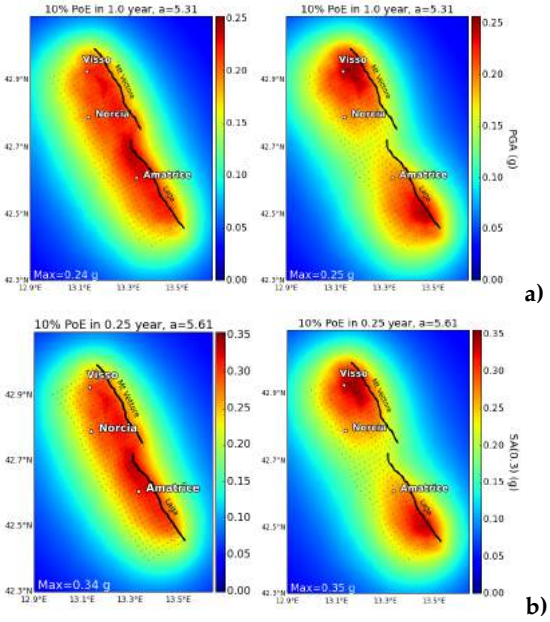

Note the effects of the inclusion of a proper fault geometry, distance metrics and of topography (Fig. 5 and ESM) in the hazard calculations: for the town of Amatrice, the aftershock hazard is slightly lower when the non-uniform

distribution of *a-values* is considered, compared to the assumption of uniform seismicity, due to the proximity of the city to the epicenter of the mainshock. We see the opposite trend, approximately same amount, for cities located at the tip ends of the fault, e.g. the town of Visso. Note also that the values obtained at 10% p.e. in 1-year since October 1, 2016 (approximately the time in which the theoretical decay is flattening, at a rate of about 2 events per day with M ≥ 1.8) are higher than the values expected in MPS04 in 50 years. Hypotheses of a more rapid decay, e.g. stated by the black curve in Fig. 4b, lead to lower values of about 20-40%.

Fig. 6 shows that the hazard curves computed in this study (APSHA) and those considered in the Italian law (MPS04) for the town of Amatrice, for both PGA and SA at 0.3s, cannot be reconciled, at least if we do not consider epistemic uncertainties of the whole logic tree. Prospective work should aim at merging APSHA with MPS04, or with updated release of the Italian reference hazard map; future efforts should include also the new information about site-effects that are being currently acquired by several institutions [www.centro microzonazionesismica.it/it/attivita/41-il-centroms-per-il-terremoto-italia-centrale-2016].

Figure 6: *hazard curves in Amatrice.*

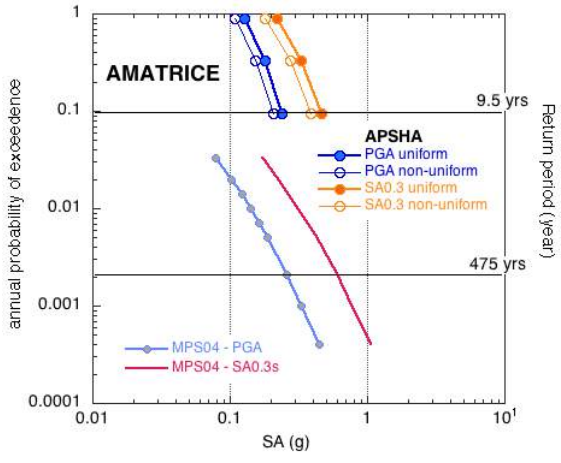

IV. Discussion

We set up a model for APSHA, in Central Italy, after the devastating event of August, 24. The theoretical approach is not novel [Yeo and Cornell, 2009; Iervolino et al., 2014], but this is the first time it has been applied in a real case in Italy, modeling aftershocks with a fault plane, within an ongoing seismic sequence. In the aim of supporting the impending recovery and rebuilding actions, we set up investigation times of 1 month/1 year since October 1st, 2016, as this is a reasonable time frame for the sequence extinction, if no triggering of nearby faults happen.

The 3D fault geometry is essentially derived from data available before the sequence, some hypothesized details have to be refined, or reshaped with a community consensus, after that more accurate data will be available. However, the introduction of a realistic fault surface and proper computation of distances from ruptures via topography leads to a hazard map that captures complexities that are as detailed as those obtained via full ground wave propagation modeling. Through a comparison of observations with event-based scenarios we are planning further analyses, in order to check to what extent this hazard map representation is realistic, and whether it can also be adopted in microzonation studies. The simple assumptions here adopted (Omori-Utsu decay of the earthquake number with time, non-uniform partitioning of seismicity rates outside the rupture area) cannot at present predict more complex fault interactions which, however, are strongly speculative: this will be an interesting aim of future work. The time-dependent seismic hazard in PGA and SA suggests that the region may experience acceleration values in the next year since October 1st that are comparable or higher to the ones stated by the Italian law in 50 years. These results cannot be extrapolated to different periods than the ones in the Omori-Utsu forecast.

This is the first time that forecasts have been made for aftershocks based on information

gathered rapidly in the wake of the mainshock. Previous knowledge of fault geometries was crucial to define the fault plane that hosted the earthquake rupture. We believe the inclusion of such information improves the forecast relative to those that do not include such information. It is particularly interesting because this unusual earthquake ruptured two separate faults as mapped at the surface. Our approach allows us to deal with this complex geometry by using realistic fault geometries that are well known in the structural geology literature where en echelon faults at surface merge downwards into a single fault at depth [Walsh et al., 1999]. A similar style of faulting may apply to other earthquakes such as the 2009 L'Aquila earthquake [Wilkinson et al., 2015], or to less known faults not as recently activated. It is worth remembering that Central Italy is often subjected to earthquake clusters, and that several faults are indicted of high time-dependent earthquake occurrence probabilities [Peruzza et al., 2011]. They motivated post L'Aquila earthquake temporary seismometric monitoring [Romano et al., 2013] in the southern Middle Aterno Valley, still silent today. In addition, the modelling of static stress variation (see Pace et al. [2014] and references therein) suggested an increase of the probability of occurrences of earthquakes in the northern Laga fault that ruptured in 2016, as well as southwards. The coupling of earthquakes on different fault segments is the main limitation of this study that we hope to overcome by this new coupling of knowledge from PSHA and structural geology. We hope this work may be an important new avenue for re-insurance companies to appreciate losses in real-time after a major earthquake as well as for research to improve disaster response.

V. EPILOGUE

On Oct 26th when the revision of this paper was near the end, a *Mw* 5.5 (data of QRMT from http://autorcmt.bo.ingv.it/quicks.html) occurred at 17:10 in the Visso area; it was compatible with the aftershock G-R and *Mmax* adopted by this study, and with the non-uniform distribution of earthquakes as given in Fig. 5. But 2 hours later, another "main" event (*Mw* 6.1) broke the northernmost patch of Mt. Vettore fault, followed on Oct 30th at 6:40 UTC by the actual biggest earthquake of the Amatrice - Mt. Vettore sequence (*Mw* 6.6). Thus, one basic assumption of this study, that no triggered and cascading events occur, does not hold anymore, as pinpointed by the reviewer, and the results provided since Oct 1st are no longer valid.

In light of the recent events, considered that the failure of a test hypothesis is itself a result, we recomputed our results for 30 days starting on Sep, 20th. This exposure period is prior to the *Mw* 6.1 earthquake of Oct 26th and posterior to the learning period of the O-U calibration. The number of *M>1.8* events increases (see Table 2) as the limits for the integration of Omori-Utsu decay curve shifts left; maximum PGA/SA values rise as well but the pattern remains the same, with maxima nearby Amatrice assuming a uniform rate distribution, and northeast of Visso in the non-uniform case. These are the results we plan to analyze under rigorous testing against real observations, in future work.

For the purpose of this special issue, we decided to keep the manuscript as it was at its first submission, with the exception of this last chapter, for the following reasons: 1) the source we designed in September, largely based on field work existing before the sequence, is still coherent with the most recent events and observations; 2) the many novelties introduced in space and time characterization of the source depict a new hazard picture, much closer to deterministic modeling than ever; 3) the time-dependency introduced for a "simplistic" decay of seismicity with no triggering of similar-sized ruptures demonstrates that the survived buildings and temporary installations after a major earthquake are statistically exposed to similar/higher shaking than those expected for long return periods. We be-

lieve this approach could be useful if applied in nearly real-time procedures, and valid in most of the sequences, as no triggered events occur. This analysis should also be a new way for identifying what a triggered event is, a debated issue in the whole scientific community.

Table 2: *APSHA, maximum PGA/SA at 10% probability of exceedance since Sep, 20th, 2016, see Table 1.*

Fault Model			PGA /SA(0.3s) (g)	
Time Sept, 20	Num M≥1.8	*a-value (a-year)*	uniform	non-uniform
30 days	932	4.769 (5.849)	0.14/0.25	0.14/0.26

ACKNOWLEDGEMENTS

For their work in the background, a special mention is due to G. Weatherill, J. Faure-Walker, S. Baize, H. Jomard. Thanks to the personell from various institutions that in labs and in the field guarantee new data acquisitions. We simpathize with the victims families and population, hoping a prompt and enduring recovery.

REFERENCES

Barchi M., F. Galadini, G. Lavecchia, P. Messina, A. M. Michetti, L. Peruzza, A. Pizzi, E. Tondi, E. Vittori (1999). Sintesi delle conoscenze sulle faglie attive in Italia Centrale: parametrizzazione ai fini della caratterizzazione della pericolosità sismica. CNR-GNDT, ftp://ftp.ingv.it/pro/gndt/Pubblicazioni/Barchi_et_alii/Barchi.htm

Benedetti L., I. Manighetti, Y. Gaudemer, R. Finkel, J. Malavieille, K. Pou, M. Arnold, G. Aumaître, D. Bourlès, and K. Keddadouche (2013). Earthquake synchrony and clustering on Fucino faults (Central Italy) as revealed from in situ 36Cl exposure dating. J. Geophys. Res. SE, 118:4948–4974, doi:10.1002/jgrb.50299.

Boncio P., G. Lavecchia, and B. Pace (2004a). Defining a model of 3D seismogenic sources for Seismic Hazard Assessment applications: the case of central Apennines (Italy). J. Seism., 8:407–425.

Boncio, P., G. Lavecchia, G. Milana, and B. Rozzi (2004b). Seismogenesis in Central Apennines, Italy: an integrated analysis of minor earthquake sequences and structural data in the Amatrice-Campotosto area. Ann. Geophys., 47:1723–1742.

Chiou B. S.J., and Youngs, R. R. (2014). Update of the Chiou and Youngs NGA model for the average horizontal component of peak ground motion and response spectra, Earthquake Spectra 30, 1117–1153.

Das S., and C. Henry (2003). Spatial relationship between main earthquake slip and its aftershock distribution, Rev. Geophys., 41(3), 1013, doi:10.1029/2002RG000119.

EMERGEO Working Group (2016). The 24 August 2016 Amatrice Earthquake: Coseismic Effects. doi: 10.5281/zenodo.61568

Galadini F., P. Galli (2003). Paleoseismology of silent faults in the Central Apennines (Italy): the Mt. Vettore and Laga Mts.Faults. Ann. Geophys., .46:815-36.

Gee R., L. Peruzza, B. Pace, R. Azzaro, S. D'Amico, and M. Pagani (2016). When probabilistic seismic hazard climbs volcanoes: how 3D topography and scaling relationships influence hazard estimates. An example from Mt. Etna (Italy) http://meetingorganizer. copernicus.org/ESC2016/ESC2016-545-1.pdf

Gruppo di Lavoro INGV (2016a). Primo rapporto di sintesi sul Terremoto di Amatrice Ml 6.0 del 24/8 2016 (Italia Centrale). doi: 10.5281/zenodo.61121

Gruppo di Lavoro sul terremoto di Amatrice (2016b). Secondo rapporto di sintesi sul Terremoto di Amatrice Ml 6.0 del 24/8/2016 (Italia Centrale). doi: 10.5281/zenodo.154400

Gruppo di lavoro IREA-CNR and INGV (2016). Sequenza sismica di Amatrice: risultati iniziali delle analisi interferometriche satellitari. doi: 10.5281/zenodo.60935

Iervolino I., Giorgio M., Polidoro B. (2014). Sequence-based probabilistic seismic hazard

analysis. Bulletin Seism Soc America, 104(2): 1006-1012

Lavecchia G., Brozzetti F., Boncio P., de Nardis R., Cirillo D. and Ferrarini F. (2016). Controllo strutturale sulla sequenza sismica di Accumoli 2016 – analisi preliminare. 80° Conv. Soc. Geol. It., www.youtube.com/watch?v=7iMos36YDcU&app=desktop

Marinkovic P. and Y. Larsen (2016). Mapping and analysis of the Central Italy Earthquake (2016) with Sentinel-1 A/B interferometry. Zenodo, doi: 10.5281/zenodo.61133

Pace B., Bocchini G.M. and Boncio P. (2014). Do static stress changes of a moderate-magnitude earthquake significantly modify the regional seismic hazard? Hints from the L'Aquila 2009 normal-faulting earthquake (Mw 6.3, central Italy). Terra Nova, 26-6: 430-439.

Pace B., Visini F. and Valentini A. (2016). 24 August 2016, Amatrice earthquake: field observations. doi: 10.13140/RG.2.2.35994.85445

Pagani M., D. Monelli, G. Weatherill, L. Danciu, H. Crowley, V. Silva, P. Henshaw, L. Butler, M. Nastasi, L. Panzeri, M. Simionato, and D. Vigano (2014). OpenQuake Engine: an open hazard (and risk) software for the Global Earthquake Model. Seism Res Lett 85:692–702.

Peruzza L., B. Pace and F. Visini (2011). Fault-Based Earthquake Rupture Forecast in Central Italy: Remarks after the L'Aquila Mw 6.3 Event. Bul Seism Soc Am, 101(1):404-412.

Piccardi L., Blumetti A.M., Comerci V., Di Manna P., Fumanti F., Guerrieri L., Leoni G., Pompili R., Vittori E, Ferrario F., Frigerio C., Livio F., Michetti A.M., Bonadeo L., Brunamonte F., Sani F., Tondi E., Wedmore L., Roberts G., Faure-Walkers J., Iezzi F., Mildon Z., Gregory L., Phillips R., Walters R., McCaffrey K., Wilkinson M., Cowie P., Rhodes E. (2016). The August 24, 2016, Amatrice earthquake (Mw 6.0): field evidence of on fault effects. http://www.isprambiente.gov.it/files/notizie-ispra/notizie-2016/sismaitaliacentrale/REPORT_Amatrice_en_2016_09_16.compressed.pdf

ReLUIS-INGV Workgroup (2016). Preliminary study of Rieti earthquake ground motion records V1.0, available at http://www.reluis.it

Roberts G. P., and A. M. Michetti (2004). Spatial and temporal variations in growth rates along active normal fault systems: An example from The Lazio–Abruzzo Apennines, central Italy. J. Struct. Geol., 26(2):339–376.

Romano M. A., R. de Nardis, M. Garbin, L. Peruzza, E. Priolo, G. Lavecchia, and M. Romanelli (2013). Temporary seismic monitoring of the Sulmona area (Abruzzo, Italy): a quality study of microearthquake locations. Nat. Hazards Earth Syst. Sci., 13:2727-44, www.nat-hazards-earth-syst-sci.net/13/2727/2013

Walsh J.J., J. Watterson, W.R. Bailey, C. Childs (1999). Fault relays, bends and branch-lines. Journal of Structural Geology 21:1019-1026.

Wilkinson M., G.P. Robert, K. McCaffrey, P.A. Cowie, J.P. Faure Walke, I. Papanikolaou, R.J. Phillips, A.M. Michetti, E. Vittori, L. Gregory, L. Wedmore, Z.K. Watson (2015). Slip distributions on active normal faults measured from LiDAR and field mapping of geomorphic offsets: an example from L'Aquila, Italy, and implications for modelling seismic moment release. Geomorphol., 237:130-41.

Yeo G.L. and C.A. Cornell (2009). A probabilistic framework for quantification of aftershock ground-motion hazard in California: Methodology and parametric study. Earth. Eng. Struct. Dyn., 38:45–60.